Published in final edited form as:

Biochim Biophys Acta Mol Basis Dis. 2019 September 01; 1865(9): 2451–2463. doi:10.1016/j.bbadis.2019.06.009.

Nicotinamide riboside, an NAD+ precursor, attenuates the development of liver fibrosis in a diet-induced mouse model of liver fibrosis

Tho X. Pham[1], **Minkyung Bae**[1], **Mi-Bo Kim**[1], **Yoojin Lee**[1], **Siqi Hu**[1], **Hyunju Kang**[1], **Young-Ki Park**[1], and **Ji-Young Lee**[1,2]

[1]Department of Nutritional Sciences, University of Connecticut, Storrs, CT 06269, USA

Abstract

Objective—Liver fibrosis is part of the non-alcoholic fatty liver disease (NAFLD) spectrum, which currently has no approved pharmacological treatment. In this study, we investigated whether supplementation of nicotinamide riboside (NR), a nicotinamide adenine dinucleotide (NAD+) precursor, can reduce the development of liver fibrosis in a diet-induced mouse model of liver fibrosis.

Methods—Male C57BL/6J mice were fed a low-fat control (LF), a high-fat/high-sucrose/high-cholesterol control (HF) or a HF diet supplemented with NR at 400 mg/kg/day (HF-NR) for 20 weeks. Features of liver fibrosis were assessed by histological and biochemical analyses. Whole-body energy metabolism was also assessed using indirect calorimetry. Primary mouse and human hepatic stellate cells were used to determine the anti-fibrogenic effects of NR in vitro.

Results—NR supplementation significantly reduced body weight of mice only 7 weeks after mice were on the supplementation, but did not attenuate serum alanine aminotransferase levels, liver steatosis, or liver inflammation. However, NR markedly reduced collagen accumulation in the liver. RNA-Seq analysis suggested that the expression of genes involved in NAD+ metabolism is altered in activated hepatic stellate cells (HSCs) compared to quiescent HSCs. NR inhibited the activation of HSCs in primary mouse and human HSCs. Indirect calorimetry showed that NR increased energy expenditure, likely by upregulation of β-oxidation in skeletal muscle and brown adipose tissue.

Conclusion—NR attenuated HSC activation, leading to reduced liver fibrosis in a diet-induced mouse model of liver fibrosis. The data suggest that NR may be developed as a potential preventative for human liver fibrosis.

[2]Corresponding author: Ji-Young Lee, Ph.D., Phone: (860) 486-1827 Fax: (860) 486-3674 ji-young.lee@uconn.edu.

Author contribution

TXP designed experiments, conducted experiments, analyzed data and wrote the manuscript. MB, MBK, YL, SH, HK, and YKP performed experiments and contributed to manuscript preparation. JYL designed experiments, analyzed and interpreted data, and wrote the manuscript.

Conflict of Interest

There is no conflict of interest to declare.

Keywords

Nicotinamide riboside; NAD+; liver fibrosis; hepatic stellate cells

1. Introduction

Non-alcoholic fatty liver disease (NAFLD) is a spectrum of disease that starts with simple steatosis and may progress towards steatohepatitis (NASH), fibrosis, and ultimately cirrhosis [1]. Development of NAFLD is strongly associated with obesity [1]. Factors such as increased adiposity and insulin resistance in obesity contribute to the progression of NASH and fibrosis [2]. Liver fibrosis was once thought to be irreversible [3]. However, it is currently accepted that liver fibrosis is reversible through the removal of the injury stimulus and the inactivation of hepatic stellate cells (HSCs), the primary cell type that produces extracellular matrix (ECM) in the liver [4, 5]. The influx of excess energy substrates from the diet and free fatty acids derived from adipose tissue to the liver primarily triggers the onset of NAFLD in obesity [6]. Therefore, in obese individuals, reduction of energy intake while increasing energy expenditure is important for the prevention of liver fibrosis.

Nicotinamide riboside (NR) is a nicotinamide adenine dinucleotide (NAD+) precursor naturally found in cow milk, where it makes up ~40% of pro-vitamin B3 [7, 8]. Studies have shown that NR attenuates weight gain and insulin resistance in obese mice by increasing energy expenditure, thus limiting the injury stimulus in the liver [9]. In both mice and humans, supplementation of NR has been demonstrated to increase cellular NAD+ levels in vitro and in vivo [9–11]. A decrease in tissue and cellular NAD+ levels has been demonstrated in several human diseases, including neurodegeneration [12], muscle dystrophy [13], and NAFLD [14]. In mice, depletion of NAD+ in fatty liver was restored with NR supplementation, decreasing hepatic fibrosis at least partly by lowering fat accumulation in the liver [15]. In humans, chronic supplementation of NR from 500–1000 mg twice a day for 6–12 weeks was well tolerated without adverse effects, although NR did not reduce body mass, body fat, or insulin resistance in middle-aged, older, and obese human adults [16, 17]. Nonetheless, NR supplementation relatively reduced hepatic lipid content by 18% in obese humans [17]. Therefore, although more studies are warranted, NR is an ideal candidate for the prevention of obesity-induced liver fibrosis.

It has been shown that NR reduced liver fibrosis in mice fed a high-fat/high-sucrose diet [15]. However, although the high-fat/high-sucrose diet-induced liver fibrosis in C57BL/6J mice, the effect was minimal. Also, this diet does not fully capture the features seen in human liver fibrosis [15, 18]. Therefore, in the present study, we fed C57BL/6J mice a high-fat/high-sucrose/high-cholesterol diet, which has been demonstrated to induce features of human liver fibrosis such as steatohepatitis, hepatocellular ballooning, and progressive fibrosis [19]. We found in this study that NR supplementation reduced liver fibrosis despite no evident reductions in steatosis and inflammation in the liver. In vitro experiments showed that NR was able to reduce HSC activation. Taken together, our data indicate that NR may be developed as an anti-fibrotic agent for the prevention of liver fibrosis in obesity.

2. Materials and Methods

2.1. Animal care and diets

Male C57BL/6J mice at the age of 7 weeks were purchased from Jackson Laboratories (Bar Harbor, ME) and were housed under a 12 h light/dark cycle. Mice at 8 weeks old were randomly assigned to a low-fat control (LF; 6% fat by wt, n=15), a high-fat/high-sucrose/high-cholesterol control (HF; 35%/34%/2.0% by wt, n=14) or a HF diet supplemented with NR at 400 mg/kg/day (HF-NR, n=14). NR was generously provided by Chromadex (Irvine, CA). Mice had *ad libitum* access to water and food throughout the 20 weeks of feeding. Body weight and food consumption were recorded weekly and plasma was collected every 4 weeks through the lateral tail vein after a 6 h fast. Oral glucose tolerance test was performed after 16 weeks on the experimental diets as described below. After 18 weeks, mice were subjected to indirect calorimetry to measure energy expenditure and physical activity as described below. In the second mouse study, C57BL/6J mice were put on a HF diet for 7 weeks to induce obesity first and then split into two groups: one staying on the HF diet (n=10), while the other was put on a HF-NR diet (n=10). The mice were subjected to indirect calorimetry at week 9, 11, and 14, corresponding to 2, 4, and 7 weeks on NR diet. At the end of the feeding period, mice were fasted for 6 h and anesthetized with ketamine (110 mg/kg)/xylazine (10 mg/kg) (Henry Schein Animal Health, Dublin, OH). Blood was collected by cardiopuncture after which the mice were euthanized through cervical dislocation before collection of the liver, epididymal white adipose tissue (eWAT), brown adipose tissue (BAT), and soleus muscle. All tissues were snap frozen in liquid nitrogen or fixed in 10% formalin. Serum and tissues were stored at −80°C until analysis. All animal procedures were approved by the Institutional Animal Care and Use Committee at the University of Connecticut.

2.2. Oral glucose tolerance test

Oral glucose tolerance was assessed in the mice after a 6 h fast. Tail blood glucose was measured using an Accu-Chek Aviva glucometer (Roche, Indianapolis, IN) at 0, 15, 30, 60, 120, and 180 mins after administration of 2 g/kg glucose by gavage [20]. The area under the curve (AUC) was calculated using GraphPad Prism 6.

2.3. Indirect calorimetry

Indirect calorimetry was performed using the Oxymax Comprehensive Lab Animal Monitoring System (CLAMS) (Columbus Instruments, OH). Mice were individually put into a CLAMS cage for a total of 72 h during which mice had access to their respective diet and water *ad libitum*. The CLAMS was located in a temperature-controlled cabinet kept at 22°C on a 12 h light/dark cycle. The first 48 h served as acclimation time for the mice and data from this period was not used for analysis. Average VO_2, VCO_2, respiratory exchange ratio (RER), heat, X-axis, and Y-axis movement were calculated by averaging all measurements in the light cycle and dark cycle during the last 24 h period [21].

2.4. Cell culture and treatment

Primary mouse HSCs were isolated from C57BL/6J mice using pronase/collagenase digestion and Nycodenz gradient as previously described [22]. Primary human HSCs were purchased from iXCells Biotechnologies (iXcells, San Diego, CA) and maintained in their proprietary media. Two days after primary mouse HSCs were plated on an uncoated dish, the cells were incubated with or without 1 mM of NR in low-glucose DMEM containing 10% FBS, 4 mM L-glutamine, 100 U/mL penicillin, and 100 μg/mL streptomycin. The cell media were changed every day until day 7. Primary human HSCs were plated on collagen-coated plates (Corning Inc, Corning, NY) overnight and then treated with 1 mM NR for 6 h. Then the cells were treated with 2 ng/mL of transforming growth factor β1 (TGFβ1) for 24 h.

2.5. Total RNA isolation and quantitative real-time PCR (qRT-PCR)

Total RNA was extracted from tissues and cells using TRIzol reagent (ThermoFisher Scientific, Waltham, MA) following the manufacturer's protocol. Reverse transcription for cDNA synthesis and qRT-PCR analysis were performed as previously described [23, 24] using Bio-Rad CFX96 Real-Time system (Bio-Rad, Hercules, CA). Primers were designed according to the GenBank database using the Beacon Designer 7 software (PREMIER Biosoft International, Palo Alto, CA) and the primer sequences are available upon request.

2.6. Western Blot Analysis

Tissue lysate was prepared as previously described [23, 24]. Antibody against α-smooth muscle actin and collagen 1α1 was purchased from MilliporeSigma (Burlington, MA). Antibody for glyceraldehyde 3-phosphate dehydrogenase was purchased from Santa Cruz Biotechnology (Dallas, TX), which was used as the loading control for data normalization. When total protein was used for normalization, REVERT Total Protein Stain (LI-COR, Lincoln, NE) was used according to manufacturer's protocol. The total protein stain was applied to the nitrocellulose membrane after protein transfer. All blots were imaged and quantified using a LI-COR Odyssey CLx (LI-COR,) and LI-COR Image Studio software.

2.7. Liver lipid extraction and serum chemistries

Liver lipids were extracted into chloroform:methanol (2:1) and solubilized in Triton X-100 as previously described [25]. Serum and liver lipids were determined enzymatically using an L-Type TG M kit (Wako chemical, Richmond, VA) for triglyceride (TG) and Cholesterol Reagent (Pointe Scientific, Canton, MI) for total cholesterol (TC). Serum glucose was measured using Liquid Glucose (Oxidase) Reagent Set (Pointe Scientific) and circulating alanine aminotransferase (ALT) activity was measured using Liquid ALT (SGPT) Reagent set (Pointe Scientific). Serum high-density lipoprotein cholesterol (HDL-C) was determined using HDL Cholesterol precipitating Reagent Set (Pointe Scientific) and serum non-HDL cholesterol (nonHDL-C) was calculated by subtracting HDL-C from TC.

2.8. Plasma lipoprotein fractionation

Size exclusion fast protein liquid chromatography was carried out on a Shimadzu Prominence high-performance liquid chromatography system (Shimadzu, Kyoto, Japan)

equipped with two Superose 6 100/300 GL column (GE Healthcare, Chicago, IL) in tandem and a SpectraChrom CF-1 fraction collector. Elution was performed in phosphate buffered saline containing 0.02% sodium azide. Mouse plasma samples were pooled for a total injection volume of 100 μL and fractionation was carried out at a flow rate of 0.2 mL/min. TC concentration of each fraction was measured as described above.

2.9. Extraction and measurement of NAD+ by enzymatic cycling assay

Extraction and measurement of NAD+ in the liver were performed as described [26]. Briefly, mouse liver frozen in liquid nitrogen was pulverized into a powder and weighed. NAD+ was extracted with ice-cold 7% perchloric acid. Supernatant from the acid-treated sample was then transferred to a new tube and neutralized with 2 M NaOH followed by 500 mM K_2HPO_4 to pH 7. NAD+ was immediately measured after extraction by enzymatic cycling assay in a black 96-well plate. For this assay, NAD+ standards (MilliporeSigma) or neutralized samples were combined with cycling assay buffer to a final concentration of 25 mM Tris pH 7.5, 5 mM $MgCl_2$, 50 mM KCl, 54 μM resazurin, 0.4 U/mL lactate dehydrogenase, and 2.25 mM L-lactate. Reactions were then initiated by the addition of diaphorase to a final concentration of 0.7 U/well. Fluorescence signal was measured every 27 s for 15 min at 530 nm excitation and 580 nm emission using a BioTek Synergy Mx (BioTek, Winooski, VT) microplate reader. The concentrations of NAD+ were determined by comparing sample slopes with those of the standards and corrected for dilutions. Results were normalized to tissue weight.

2.10. Liver histology

Formalin-fixed liver samples were paraffin embedded, sectioned, and stained with hematoxylin and eosin (H&E) or Gömöri trichrome at the Connecticut Veterinary Medical Diagnostic Laboratory (CVMLD), the University of Connecticut. Also, paraffin-embedded liver sections were subjected to Picrosirius red staining. Slides were first deparaffinized and rehydrated by immersion in xylene twice for 5 min, followed by 100% ethanol twice for 5 min. The slides were then immersed through graded ethanol (95%, 70%, 50%) for 5 min each and finally in water for 5 min. Subsequently, the slides were stained with Weigert's iron hematoxylin (Electron Microscopy Sciences, Hatfield, PA) for 8 min and then washed with water for 10 min, after which they were stained with picrosirius red staining solution (0.1% (w/v) Direct red 80 (MilliporeSigma) in saturated aqueous picric acid (Ricca Chemicals, Arlington, TX)) for 2 h. Slides were then washed with acidified water for 1 min and then twice with 100% ethanol for 5 min. After washing the slides with xylene for 5 min, the stained sections were covered with a coverslip using a DPX mountant (MilliporeSigma), air-dried, and imaged. Picrosirius red positive area was then calculated using Image J image analysis software. All stained images were captured with a 10X objective using the Zeiss Axio Vert A1 (Oberkochen, Germany) equipped with an MRc camera.

2.11. Total collagen measurement

Total collagen was measured using a Quickzyme Total Collagen Assay kit (Quickzyme, The Netherlands) following the manufacturer's protocol. The assay is based on the detection of hydroxyproline. Briefly, a portion of liver tissue samples homogenized in water was used for generating the hydrolysate, and another portion was stored at −80°C for subsequent protein

quantification. Liver hydrolysates were then generated by the addition of 12 M HCl to an equal volume of the homogenates to a final concentration of 6 M HCl and heated at 95°C for 20 h. Total collagen levels of the hydrolysate were then measured according to the manufacturer's protocol, and results were normalized to total protein content.

2.12. RNA sequencing and data analysis

RNA sequencing and data analysis were done as previously [27]. Briefly, mouse primary HSCs were isolated as mentioned above and plated onto uncoated dishes. After one day, total RNA was isolated to represent quiescent HSCs (qHSCs). Total RNA was also isolated from another set of cells kept until day 7 with media change every day to represent activated HSCs (aHSCs). The entire process was repeated 3 additional times, for a total of 4 replicates from 4 different mice. Total RNA was subjected to RNA-Seq analysis as described previously.

2.13. Statistical Analysis

One-way ANOVA with Tukey's post-hoc analysis or Student's t-test was used to detect significant differences of treatments with $P < 0.05$ considered significant by GraphPad Prism 6 (GraphPad Software Inc., La Jolla, CA). Data are expressed as mean ± SEM.

3. Results

3.1. NR supplementation lowered body weight and led to a more favorable lipid profile in the circulation, but did not improve glucose tolerance

The average body weights of mice in the HF group was significantly higher than those of the LF control, but NR significantly attenuated weight gains of mice starting at 7 weeks (Figure 1A). After 20 weeks of experimental diets, the LF group had the lowest body weight gain, followed by the HF-NR group, while the HF group gained the most weight (Figure 1B). Reduction of body weight was not due to differences in food consumption between the HF and HF-NR group, as both ate a similar amount of food throughout the study (data not shown). Reduction of body weight gain with NR supplementation is consistent with other studies [9, 11].

Fasting serum TC concentrations were significantly increased by the HF diet compared to the LF diet, but this increase was significantly attenuated in the HF-NR group (Figure 1C). Circulating nonHDL-C, primarily LDL-C, and HDL-C levels were significantly higher in the HF than the LF control. While NR supplementation did not alter nonHDL-C, it ablated the increase in HDL-C levels. Although terminal serum nonHDL-C concentrations were not significantly lowered in the HF-NR group, FPLC analysis of plasma samples at 12 and 16 weeks for lipoprotein distribution demonstrated a clear reduction in cholesterol in the LDL fraction (Figure 1D). Serum TG concentrations were not significantly different between the LF and HF group, but they were significantly lower in the HF-NR group than the LF control (Figure 1E). Serum glucose levels of the HF and HF-NR groups were significantly increased compared to the LF group but were not significantly different from each other (Figure 1F). Both the HF and the HF-NR groups were less glucose tolerant compared to the LF group, with no significant difference between them (Figure 1G & H). Together, our data suggest

that supplementation of NR reduced body weight gain and attenuated diet-induced dyslipidemia but had minimal effects on hyperglycemia and glucose tolerance.

3.2. NR did not reduce TG and TC accumulation or inflammation in the liver

The liver weights of the HF and HF-NR groups were significantly higher than those of the LF group, but they were not significantly different from each other (Figure 2A). A similar trend was seen for hepatic TG and TC levels (Figure 2B). Plasma levels of ALT, a marker of liver injury [28], were significantly elevated after 4 weeks on the HF or HF-NR diet compared to the LF diet, but there was no significant difference between HF and HF-NR (Figure 2C). Of note, circulating ALT levels were progressively increased throughout the feeding period, reaching their peak at 16 weeks. Consistent with our observation, it has been reported that in chronic hepatic injury, ALT is commonly elevated, but as fibrosis progresses, ALT activity typically declines [29, 30]. Staining of liver sections with H&E showed noticeable accumulation of lipids in the liver of HF and HF-NR groups compared to the LF group, but NR supplementation did not reduce liver lipids compared to the HF group (Figure 2D), supporting our results of liver weights and lipids. However, hepatic expression of genes related to lipid metabolism genes, such as sterol regulatory element-binding protein 1C (*Srebp1c*) and fatty acid synthase (*Fas*), showed a significant reduction in the HF-NR group compared to the HF (Supplemental Table 1).

Hepatic expression of macrophage markers, such as EGF-like module-containing mucin-like hormone receptor-like 1 (*Emr1*), and chemoattractant chemokine (C-C motif) ligand 2 (*Ccl2*), was significantly elevated in both the HF and the HF-NR compared to the LF group (Figure 2E). Similarly, mRNA levels of inflammatory genes, i.e., interleukin-1β (*Il-1b*) and tumor necrosis factor α (*Tnfa*), were elevated in both the HF and HF-NR group, however, the HF-NR group was significantly different from the HF group. Our data suggest that the livers of the HF and HF-NR group likely experienced similar levels of lipotoxic stress as evidenced by no significant differences in their expression of hepatic inflammatory genes and ALT release into the blood.

3.3. NR supplementation reduced collagen accumulation in the liver

We next assessed the effect of NR supplementation on the development of liver fibrosis. Liver trichrome and picrosirius red stainings, which visualize collagen in blue and red, respectively, suggest that HF markedly increased the accumulation of collagen in the liver compared to that of LF, while NR supplementation noticeably attenuated collagen accumulation (Figure 3A). Quantification of the Picrosirius red-positive area showed significant increases in the liver of HF-fed mice, which were significantly attenuated by NR (Figure 3B). To corroborate the histological data, total collagen was measured in the liver based on the detection of hydroxyproline [31]. HF significantly increased collagen in the liver compared to LF group, while NR supplementation significantly attenuated the increase to a similar level as the LF (Figure 3C). Mice on the HF diet had higher mRNA levels of fibrotic markers, such as α-smooth muscle actin (*Acta2*), collagen 1α1 (*Col1a1*), and *Col6a1*, which were significantly attenuated by NR supplementation (Figure 3D). There were marked increases in COL1α1 protein levels by HF, which was significantly attenuated in the HF-NR group (Figure 3E & F). The results demonstrated that NR supplementation

attenuated the development of liver fibrosis in this mouse model of diet-induced liver fibrosis.

3.4. HF altered liver NAD+ metabolism, which was attenuated by NR supplementation

As NR is an NAD+ precursor, we investigated the effect of NR supplementation on the hepatic NAD+ metabolism. HF significantly reduced NAD+ levels in the liver, but NR supplementation was able to significantly attenuate the decrease (Figure 4A). To gain insight into the changes in NAD+ levels by HF and HF-NR, we measured the expression of well-known NAD+-consuming enzymes and enzymes of the NAD+ salvage pathway [32–34]. The hepatic expression of the NAD+ consumers, i.e., poly (ADP-Ribose) polymerase 1 (*Parp1*) and sirtuin 1 (*Sirt1*), was not altered in all groups, while the expression of another NAD+ consumer *Cd38* was significantly increased in the HF and HF-NR groups compared to the LF group (Figure 4B). Both PARP1 and SIRT1 have been demonstrated to consume ~1/3 of cellular NAD+ by cleaving the ADP-ribose moiety from NAD+ and transferring it to an acceptor protein or cleaving the ADP-ribose moiety and transferring an acetyl group to it, respectively [35–37]. The NAD+-consuming enzyme, CD38 cleaves NAD+ to make the secondary calcium messenger cyclic ADP-ribose [38]. Nicotinamide phosphoribosyltransferase (NAMPT) is responsible for the conversion of nicotinamide to nicotinamide mononucleotide (NMN) both intracellularly and extracellularly [39]. The enzyme CD73 converts NMN to NR [40]. The enzyme nicotinamide riboside kinase 1 (NMRK1) phosphorylates intracellular NR to produce NMN, while nicotinamide mononucleotide adenylyltransferases (NMNAT) is responsible for the regeneration of NAD+ from NMN [41]. The expression of *Nampt* was significantly increased in the HF group compared to the LF group, while NR supplementation further increased its expression (Figure 4C). The expression of *Cd73* was significantly increase by HF compared to LF, which was attenuated by NR supplementation. However, the expression of *Nmnat1* was not significantly different between the three groups. The expression of *Nmrk1* and *Nmnat3* was significantly changed by HF compared to LF to opposite directions, but only change in *Nmrk1* expression was significantly attenuated by NR supplementation. Furthermore, NAD+ levels in the liver were negatively correlated to the levels of hepatic collagen, TC, and TG (Figure 4D), suggesting that NAD+ levels may be an important determinant of collagen, cholesterol, and TG accumulation in the liver. The results suggest that HF diet-induced changes in NAD+ metabolism in the liver, leading to a significant reduction in NAD+ levels and that NR supplementation was able to partially attenuate these changes.

3.5. NAD+ metabolism was altered in activated HSCs and NR treatment attenuated the activation of HSCs

HSCs are the primary ECM-producing cell type in the liver [4, 5]. To investigate whether NAD+ metabolism is altered in qHSCs and aHSCs, RNA-Seq analysis was performed with primary mouse HSCs in a quiescent (day 1) and an activated state (day 7). The expression of genes whose function requires the binding of NAD+ as a cofactor was markedly different between qHSCs and aHSCs (Figure 5A). Furthermore, the majority of genes important for de novo biosynthesis of NAD+, including the NAD salvage pathway, were down-regulated in aHSCs compared to qHSCs (Figure 5B). In particular, mRNA levels of *Nampt* and *Nmrk1*, as assessed by qRT-PCR, confirmed that *Nampt* was repressed while *Nmrk1* was

upregulated in aHSCs (Figure 5C). We next investigated whether NR treatment can alter the activation of HSCs. Treatment of 1 mM of NR during the activation of primary mouse HSCs significantly reduced the expression of the activation marker, i.e., *Acta2* and *Col1a1*, compared to untreated aHSCs (Figure 5D). Consistently, NR decreased both αSMA and COL1α1 protein levels compared to untreated aHSCs (Figure 5E). TGFβ1 is a pro-fibrogenic cytokine that can activate HSCs and is commonly elevated in the fibrotic liver [42]. We next tested whether NR treatment can attenuate the activation of primary human HSCs by TGFβ1. TGFβ1 significantly increased the expression of *ACTA2* and *COL1A1* in primary human HSCs and treatment with NR was able to significantly reduce the expression of *ACTA2*, but not *COL1A1* (Figure 5F). However, at the protein level, NR treatment reduced both αSMA and COL1α1 induced by TGFβ1 in primary human HSCs (Figure 5G). Our data suggest that NAD+ metabolism was altered when qHSCs becomes activated and that NR inhibited HSC activation.

3.6. NR did not alter the expression of genes involved in energy utilization in eWAT but reduced its weight

As body weight gain was reduced by NR supplementation, we next evaluated the effect of NR on eWAT. The eWAT weights of the HF-NR group were significantly lower than those of the HF group (Figure 6A). To explain the significant decrease in eWAT weight by NR, we measured the expression of genes important for adipose tissue function and lipid oxidation. The HF diet significantly reduced the mRNA expression of peroxisome proliferator-activated receptor γ (*Pparg*), perilipin (*Plin1*) and adiponectin (*Adipoq*) compared to the LF group, while NR significantly attenuated this effect in *Adipoq* and trended toward an increase in *Pparg* (Figure 6B). Genes for lipid oxidation was not significantly changed in eWAT between HF and HF-NR (data not shown). H&E staining of eWAT sections showed noticeable crown-like structures (CLS), which are macrophages surrounding dead adipocytes [43], in both HF and HF-NR groups compared to the LF, but CLS did not differ from each other (Figure 6C). There were significant increases in the expression of *Emr1*, a macrophage marker, in the eWAT of both the HF and HF-NR group which supports the histological results (Figure 6D). Collectively, the data suggest that the eWAT of mice supplemented with NR showed less metabolic stress than those of the HF group based on *Pparg* and *Adipoq* expression, however, there were no significant changes in energy metabolism and inflammation in this fat depot by NR.

3.7. NR increased whole body energy utilization in mice

To investigate whether the reduction of body weight in the NR-fed mice was due to an increase in energy expenditure, indirect calorimetry was used to measure oxygen consumption, carbon dioxide production, and physical activity of mice. On average the rates of oxygen consumption and carbon dioxide production of mice on the LF diet was higher than those of the HF and HF-NR groups (Figure 7A & B). VO_2 values during the light cycle were higher in the HF-NR group compared to the HF group, while there were no differences in the VCO_2 between the two groups in both cycles (Figure 7B). There were no significant differences in physical activity between the HF and HF-NR groups, although mice in the HF-NR group used the running wheel significantly more often than mice on the HF diet (Figure 7C & D). There was no significant difference in respiratory exchange ratio (RER)

between the HF and HF-NR groups, indicating that both groups predominately used lipids as their primary energy source (Figure 7E). Energy expenditure determined by heat production was significantly higher in the HF-NR group compared to the HF in the light cycle, while in the dark cycle it was not significant although there was an increasing trend with NR supplementation (Figure 7F).

To determine if NR supplementation can increase energy expenditure prior to significant changes in body weight, we measured energy expenditure of mice 2 weeks, 4 weeks, and 7 weeks after NR supplementation. Significant body weight change did not occur until 8 weeks of NR supplementation (Supplemental Figure 1A). After 2 weeks of NR supplementation, there was no difference in the energy expenditure (Supplemental Figure 1B). However, after 4 weeks and continuing until after the 7th week on NR feeding, noticeable changes in energy expenditure in the HF-NR group were observed compared to the HF group, which was trending toward significance (Supplemental Figure 1C). Our results suggest that increased energy expenditure by NR likely contributes to attenuated weight gain in mice.

3.8. NR increased the expression of genes responsible for energy utilization in soleus muscle and BAT

To investigate whether the increase in whole-body energy expenditure by NR was due to increased metabolism in skeletal muscle and BAT, we measured the mRNA expression of genes important for lipid oxidation and mitochondria biogenesis in these tissues. In the soleus muscle, despite a significant reduction in mRNA levels of PPARγ coactivator 1α (*Ppargc1a*) in the HF-NR group compared to the LF group, the expression of mitochondria transcription factor A (*Tfam*), carnitine palmitoyltransferase 1β (*Cpt1b*), uncoupling protein 2 (*Ucp2*), and citrate synthase (*Cs*) was significantly increased in the HF-NR group compared to the LF and the HF groups (Figure 8A). Furthermore, there was a significant increase in mitochondrial DNA in the soleus muscle of the HF-NR group compared to that of the LF and HF groups (Figure 8B).

In BAT, the expression of *Cpt1a*, peroxisomal acyl-coenzyme A oxidase 1 (*Acox1*), and Glucose transporter 4 (*Slc2a4*) was significantly higher in the HF-NR group than the HF and LF groups (Figure 8C). Mitochondrial DNA in BAT was significantly increased in both the HF and HF-NR groups compared to the LF group but was not significantly different from each other (Figure 8D).

4. Discussion

To date, no single therapy has been approved for treating NAFLD, and few treatments for NASH exist [44]. Given the chronic nature of the development of NASH and liver fibrosis, lifestyle changes and dietary means are important for the prevention of diseases. Here we showed that supplementation of NR, an NAD+ precursor, attenuated the development of liver fibrosis in mice fed a diet that has been demonstrated to produce progressive fibrosis similar to those in humans [19]. The protective effect of NR on liver fibrosis was independent of changes in liver steatosis and inflammation in obesity. In addition, the present study provided evidence that NAD+ metabolism is altered in the transition of HSCs

from a quiescent state to an activated state, which can be attenuated by NR with inhibition of HSC activation.

Liver fibrosis is the result of chronic activation of wound healing in response to liver injury [45, 46]. In the present study, plasma levels of ALT, which leak out into the circulation from hepatocytes upon injury [28], were similar in HF and HF-NR groups, suggesting that hepatocytes within the liver were equally injured in these groups. It is presumable that the liver of the HF and HF-NR groups might experience a similar degree of lipotoxic stress induced by the diet rich in fat, sucrose, and cholesterol based on no differences in their hepatic accumulation of TG and TC. The liver injury typically results in inflammation and recruitment of immune cells from the circulation [47]. Hepatic expression of inflammatory genes including *Ccl2*, *Emr1, Il1b* and *Tnfa* was not different between the HF and HF-NR groups, suggesting that NR supplementation did not alter macrophage infiltration into the liver or their expression of cytokines. As the degree of liver injury and inflammation is in line with that of liver fibrosis, we did not expect to see a significant effect of NR on the development of liver fibrosis. However, picrosirius red and trichrome staining, collagen accumulation, and mRNA expression of fibrogenic genes in the liver demonstrated a significant reduction in liver fibrosis by NR supplementation. Therefore, the data support that NR supplementation reduces the development of liver fibrosis independent of steatosis and inflammation in this mouse model of obesity-associated liver fibrosis. As HSCs are the primary producer of ECM during liver injury, our data suggest that NR may have a direct effect on HSCs.

Crucial roles of HSCs in the development of liver fibrosis have been well supported in animal and human studies [4, 5, 46]. Upon liver damage, qHSCs transdifferentiate into αSMA-positive aHSCs that secrete ECM substances while inhibiting their breakdown, leading to collagen accumulation in the liver [45]. A variety of cytokines released by immune cells, such as TGFβ1, or by damaged hepatocytes may activate HSCs [45, 48]. We showed that treatment of NR during the activation of primary mouse HSCs in a quiescent state repressed the expression of *Acta2* and *Col1a1*, suggesting that NR inhibits the transdifferentiation of qHSCs to aHSCs. Also, we demonstrated that NR treatment attenuated the induction of *ACTA2* and *COL1A1* by TGFβ1 in primary human HSCs. Previously, Gariani et al. [15] showed that NR supplementation reduced liver fibrosis. In that study, NR supplementation significantly reduced plasma ALT, liver steatosis, and liver inflammation, such that it is difficult to know whether the attenuation of fibrosis by NR is primary or secondary to the reductions in steatosis and inflammation. In contrast, the present study demonstrates that NR can attenuate the development of liver fibrosis in vivo without altering steatosis and inflammation in the liver, which may be attributable to its direct inhibition of HSC activation. The direct inhibition of HSCs by NR supplementation in vivo remains to be determined.

A notable difference between the present study and Gariani et al. [15] is the effect of NR on liver steatosis. This could be due to the inclusion of a high amount of cholesterol in our diet compared to theirs. It has been demonstrated that high dietary cholesterol in mice can increase hepatic free cholesterol accumulation in mitochondria and induces mitochondria dysfunction [49]. One of the central findings of Gariani et al. is that NAD+ repletion by NR

supplementation induces the mitochondria unfolded protein response, which leads to reduced steatosis [15]. Therefore, it is possible that in our current study, the addition of high cholesterol in the diet may lead to an impairment of the mitochondria unfolded protein response and hence, a lack of NR effect on liver steatosis. In support of this speculation, we did not observe any increases by NR in the expression of genes for β-oxidation and mitochondrial biogenesis as well as mitochondrial DNA copy number in the liver (data not shown), all of which were increased by NR supplementation in their study.

The role of NAD+ in the activation of HSCs has not been studied before. Our RNA-Seq analysis suggests that the expression of enzymes that require NAD+ as a cofactor was altered when qHSCs became activated. Furthermore, the majority of genes for the de novo NAD+ biosynthesis pathway, such as tryptophan 2,3-dioxygenase and kynureninase, and the NAD+ salvage pathway, such as *Nampt*, were downregulated in aHSCs compared with qHSCs. A recent study using an isotope-tracer demonstrated that cells in culture, with the exception of primary hepatocytes, do not typically synthesize NAD+ from tryptophan and depend entirely on nicotinamide for their NAD+ [35]. This study suggests that NAD+ levels in cultured cells are highly dependent on the NAD salvage pathway, where NAMPT is the rate-limiting enzyme [50]. Indeed, another recent study identified NAMPT as a differentially expressed protein in human HSCs, where it is significantly reduced in aHSCs [51]. This is consistent with our data that *Nampt* expression was significantly reduced in activated primary mouse HSCs. Collectively, our data suggest that NAD+ metabolism may be altered in aHSCs due to the repression of NAMPT. Future research into the role of NAMPT in the activation of HSCs is warranted.

In the current study, of several NAD+ consuming enzymes, only liver CD38 expression was significantly increased by the HF and HF-NR diet. However, Western blot analysis showed that CD38 protein level was significantly reduced in both the HF and HF-NR group (data not shown). This suggest that CD38 may not be responsible for the reduction of liver NAD+ in response to a high-fat diet. In fact, it has been demonstrated that genetic deletion and pharmacological inhibition of PARP1 can significantly attenuate the reduction of liver NAD + induced by a high-fat diet [52, 53]. These studies support the notion that PARP1 and its activity may be the biggest determinant of liver NAD+ levels in response to a high-fat diet.

It is not entirely clear how increased cellular NAD+ levels would inhibit the activation of HSCs. However, it has been demonstrated that enzymes consuming NAD+, such as PARP1 and CD38, play an important role in HSC activation, where whole-body deletion of either enzyme in mice inhibits HSC activation and liver fibrosis [54, 55]. One critical consequence of increased NAD+ levels is the activation of SIRT1 [9]. Several studies have shown that SIRT1 expression is down-regulated in the fibrotic liver and aHSCs [56–58]. Furthermore, in vitro overexpression of *Sirt1* was able to attenuate the activation of HSCs [56, 58]. Mechanistically, the acetylation of SMAD3, which is a downstream mediator of the TGFβ1 signaling [59], leads to the enhanced binding of SMAD3 to the promoters of its target genes [60, 61]. In contrast, the activation of SIRT1 in HSC-T6 HSCs has been demonstrated to deacetylate SMAD3, inhibiting its binding to the promoters of *Col1α1* and *Acta2* [57]. Therefore, the activation of SIRT1 in HSCs by NR may be responsible for the inhibition of HSC activation observed in our in vitro experiments. While we did not detect significant

differences in the expression of *Sirt1* in the livers of the HF and HF-NR groups, it is possible that SIRT1 activity in the liver may be higher in the HF-NR than the HF group. Furthermore, the expression of *Sirt1* and its activity in the liver may not reflect those of HSCs, as HSCs make up ~15% of the total number of resident cells in the liver [45]. In the future, it will be important to isolate HSCs from NR-fed mice to better understand the effect of NR on SIRT1 activation.

NR supplementation reduced body and eWAT weights, which is consistent with other studies [9, 11, 15]. The increased energy expenditure in the HF-NR group compared with the HF group is likely responsible for the decreases in body and eWAT weights. The present study suggests that fatty acid β-oxidation may be enhanced in BAT and skeletal muscle by NR, indicating that these two metabolically active tissues are the principal tissues responsible for the dissipation of energy by NR. Interestingly, it has been demonstrated that skeletal muscle preferentially takes up NR as an NAD+ precursor compared to nicotinamide mononucleotide and nicotinamide [35]. Together our data suggest that NR may uniquely affect energy metabolism in skeletal muscle to decrease weight gain. Of significance, to avoid the confounding effect of body weight on energy expenditure, we showed that NR was able to increase the energy expenditure of the mice prior to significant changes in their body weight. Therefore, energy expenditure is likely increased due to NR supplementation but not due to changes in body weight.

In conclusion, we demonstrated that supplementation of NR in a diet-induced model of liver fibrosis increased energy expenditure to prevent body weight gain and inhibited the development of liver fibrosis independent of steatosis and inflammation. Also, the present study shows for the first time that NAD+ metabolism is markedly different between qHSCs and aHSCs, and that NR treatment attenuated HSC activation, suggesting that NR may prevent the development of liver fibrosis by directly affecting the activation process of HSCs. Therefore, future studies directly investigating the role of NR and NAD+ on the activation of HSCs are warranted. Furthermore, NR should be developed as a potential preventative to inhibit the development of liver fibrosis in humans.

Supplementary Material

Refer to Web version on PubMed Central for supplementary material.

Acknowledgments

We thank Chromadex for providing nicotinamide riboside for this study.

Funding Source: This study was supported by NIH 3R01DK108254–04S1 and USDA Multistate Hatch CONS00992 and CONS00916 to J. Lee; and USDA AFRI 2016–08864 and USDA Hatch CONS00978 to Y. Park.

Abbreviations

ACOX1	peroxisomal acyl-coenzyme A oxidase 1
Adipoq	adiponectin
ALT	alanine aminotransferase

AUC	area under the curve
αSMA	α smooth muscle actin
BAT	brown adipose tissue
CLAMS	comprehensive lab animal monitoring system
Col1α1	collagen 1α1
CPT1	carnitine palmitoyltransferase 1
CS	citrate synthase
eWAT	epididymal white adipose tissue
H&E	hematoxylin & eosin
HDL-C	high-density lipoprotein cholesterol
HSC	hepatic stellate cell
LDL-C	low-density lipoprotein cholesterol
NAD	nicotinamide adenine dinucleotide
NAFLD	nonalcoholic fatty liver disease
NASH	nonalcoholic steatohepatitis
NMNAT	nicotinamide mononucleotide adenylyltransferase
NR	nicotinamide riboside
NRK1	nicotinamide riboside kinase 1
Plin1	perilipin 1
PPARγ	peroxisome proliferator-activated receptor γ
PPARGC1A	PPARγ coactivator 1 alpha
Sirt1	Sirtuin 1
SLC2A4	solute carrier family 2 member 4
TNFα	tumor necrosis factor α
OGTT	oral glucose tolerance test
RER	respiratory exchange ratio
TGFβ1	transforming growth factor β1
Emr1	EGF-like module-containing mucin-like hormone receptor-like 1
IL1β	interleukin-1β

CCL2	C-C motif chemokine ligand 2

References

[1]. Hardy T, Oakley F, Anstee QM, Day CP. Nonalcoholic Fatty Liver Disease: Pathogenesis and Disease Spectrum. Annu Rev Pathol. 2016;11:451–96. [PubMed: 26980160]

[2]. Chiang DJ, Pritchard MT, Nagy LE. Obesity, diabetes mellitus, and liver fibrosis. Am J Physiol Gastrointest Liver Physiol. 2011;300:G697–702. [PubMed: 21350183]

[3]. Pellicoro A, Ramachandran P, Iredale JP. Reversibility of liver fibrosis. Fibrogenesis Tissue Repair. 2012;5:S26. [PubMed: 23259590]

[4]. Troeger JS, Mederacke I, Gwak GY, Dapito DH, Mu X, Hsu CC, et al. Deactivation of hepatic stellate cells during liver fibrosis resolution in mice. Gastroenterology. 2012;143:1073–83 e22. [PubMed: 22750464]

[5]. Kisseleva T, Cong M, Paik Y, Scholten D, Jiang C, Benner C, et al. Myofibroblasts revert to an inactive phenotype during regression of liver fibrosis. Proc Natl Acad Sci U S A. 2012;109:9448–53. [PubMed: 22566629]

[6]. Fabbrini E, Sullivan S, Klein S. Obesity and nonalcoholic fatty liver disease: biochemical, metabolic, and clinical implications. Hepatology. 2010;51:679–89. [PubMed: 20041406]

[7]. Bieganowski P, Brenner C. Discoveries of nicotinamide riboside as a nutrient and conserved NRK genes establish a Preiss-Handler independent route to NAD+ in fungi and humans. Cell. 2004;117:495–502. [PubMed: 15137942]

[8]. Trammell SA, Yu L, Redpath P, Migaud ME, Brenner C. Nicotinamide Riboside Is a Major NAD+ Precursor Vitamin in Cow Milk. J Nutr. 2016;146:957–63. [PubMed: 27052539]

[9]. Canto C, Houtkooper RH, Pirinen E, Youn DY, Oosterveer MH, Cen Y, et al. The NAD(+) precursor nicotinamide riboside enhances oxidative metabolism and protects against high-fat diet-induced obesity. Cell Metab. 2012;15:838–47. [PubMed: 22682224]

[10]. Trammell SA, Schmidt MS, Weidemann BJ, Redpath P, Jaksch F, Dellinger RW, et al. Nicotinamide riboside is uniquely and orally bioavailable in mice and humans. Nat Commun. 2016;7:12948. [PubMed: 27721479]

[11]. Trammell SA, Weidemann BJ, Chadda A, Yorek MS, Holmes A, Coppey LJ, et al. Nicotinamide Riboside Opposes Type 2 Diabetes and Neuropathy in Mice. Sci Rep. 2016;6:26933. [PubMed: 27230286]

[12]. Verdin E NAD(+) in aging, metabolism, and neurodegeneration. Science. 2015;350:1208–13. [PubMed: 26785480]

[13]. Ryu D, Zhang H, Ropelle ER, Sorrentino V, Mazala DA, Mouchiroud L, et al. NAD+ repletion improves muscle function in muscular dystrophy and counters global PARylation. Sci Transl Med. 2016;8:361ra139.

[14]. Zhou CC, Yang X, Hua X, Liu J, Fan MB, Li GQ, et al. Hepatic NAD(+) deficiency as a therapeutic target for non-alcoholic fatty liver disease in ageing. Br J Pharmacol. 2016;173:2352–68. [PubMed: 27174364]

[15]. Gariani K, Menzies KJ, Ryu D, Wegner CJ, Wang X, Ropelle ER, et al. Eliciting the mitochondrial unfolded protein response by nicotinamide adenine dinucleotide repletion reverses fatty liver disease in mice. Hepatology. 2016;63:1190–204. [PubMed: 26404765]

[16]. Martens CR, Denman BA, Mazzo MR, Armstrong ML, Reisdorph N, McQueen MB, et al. Chronic nicotinamide riboside supplementation is well-tolerated and elevates NAD(+) in healthy middle-aged and older adults. Nat Commun. 2018;9:1286. [PubMed: 29599478]

[17]. Dollerup OL, Christensen B, Svart M, Schmidt MS, Sulek K, Ringgaard S, et al. A randomized placebo-controlled clinical trial of nicotinamide riboside in obese men: safety, insulin-sensitivity, and lipid-mobilizing effects. Am J Clin Nutr. 2018;108:343–53. [PubMed: 29992272]

[18]. Ishimoto T, Lanaspa MA, Rivard CJ, Roncal-Jimenez CA, Orlicky DJ, Cicerchi C, et al. High-fat and high-sucrose (western) diet induces steatohepatitis that is dependent on fructokinase. Hepatology. 2013;58:1632–43. [PubMed: 23813872]

[19]. Charlton M, Krishnan A, Viker K, Sanderson S, Cazanave S, McConico A, et al. Fast food diet mouse: novel small animal model of NASH with ballooning, progressive fibrosis, and high physiological fidelity to the human condition. Am J Physiol Gastrointest Liver Physiol. 2011;301:G825–34. [PubMed: 21836057]

[20]. Lee Y, Pham TX, Bae M, Hu S, O'Neill E, Chun OK, et al. Blackcurrant (Ribes nigrum) Prevents Obesity-Induced Nonalcoholic Steatohepatitis in Mice. Obesity (Silver Spring). 2019;27:112–20. [PubMed: 30569636]

[21]. Tho X Pham YL, Minkyung Bae, Siqi Hu, Hyunju Kang, Mi-Bo Kim, Young-Ki park, Ji-Young Lee. Spirulina supplementation in a mouse model of diet-induced liver fibrosis reduced the pro-inflammatory response of splenocytes. British Journal of Nutrition. 2018.

[22]. Yang Y, Bae M, Park YK, Lee Y, Pham TX, Rudraiah S, et al. Histone deacetylase 9 plays a role in the antifibrogenic effect of astaxanthin in hepatic stellate cells. J Nutr Biochem. 2017;40:172–7. [PubMed: 27915160]

[23]. Park YK, Rasmussen HE, Ehler SJ, Blobaum KR, Lu F, Schlegel VL, et al. Repression of proinflammatory gene expression by lipid extract of Nostoc commune var sphaeroides Kutzing, a blue-green alga, via inhibition of nuclear factor-kappa B in RAW 264.7 macrophages. Nutr Res. 2008;28:83–92. [PubMed: 19083393]

[24]. Rasmussen HE, Blobaum KR, Park YK, Ehlers SJ, Lu F, Lee JY. Lipid extract of *Nostoc commune var. sphaeroides Kutzing*, a blue-green alga, inhibits the activation of sterol regulatory element binding proteins in HepG2 cells. J Nutr. 2008;138:476–81. [PubMed: 18287352]

[25]. Park YK, Rasmussen HE, Ehlers SJ, Blobaum KR, Lu F, Schlegal VL, et al. Repression of proinflammatory gene expression by lipid extract of Nostoc commune var sphaeroides Kutzing, a blue-green alga, via inhibition of nuclear factor-kappaB in RAW 264.7 macrophages. Nutr Res. 2008;28:83–91. [PubMed: 19083393]

[26]. Li W, Sauve AA. NAD(+) content and its role in mitochondria. Methods Mol Biol. 2015;1241:39–48. [PubMed: 25308486]

[27]. Minkyung Bae TXP, Young-Ki Park, Yoojin Lee, Siqi Hu, Dong-Guk Shin, Pujan Joshi, Seung-Hyun Hong, Nathan Alder, Koo Sung I., Lee Ji-Young. Metabotypic changes of hepatic stellate cells during activation are attenuated by astaxanthin Scientific Report. 2019.

[28]. Kim WR, Flamm SL, Di Bisceglie AM, Bodenheimer HC, Public Policy Committee of the American Association for the Study of Liver D. Serum activity of alanine aminotransferase (ALT) as an indicator of health and disease. Hepatology. 2008;47:1363–70. [PubMed: 18366115]

[29]. Williams AL, Hoofnagle JH. Ratio of serum aspartate to alanine aminotransferase in chronic hepatitis. Relationship to cirrhosis. Gastroenterology. 1988;95:734–9. [PubMed: 3135226]

[30]. Sheth SG, Flamm SL, Gordon FD, Chopra S. AST/ALT ratio predicts cirrhosis in patients with chronic hepatitis C virus infection. Am J Gastroenterol. 1998;93:44–8. [PubMed: 9448172]

[31]. Qiu B, Wei F, Sun X, Wang X, Duan B, Shi C, et al. Measurement of hydroxyproline in collagen with three different methods. Mol Med Rep. 2014;10:1157–63. [PubMed: 24858249]

[32]. Bogan KL, Brenner C. Nicotinic acid, nicotinamide, and nicotinamide riboside: a molecular evaluation of NAD+ precursor vitamins in human nutrition. Annu Rev Nutr. 2008;28:115–30. [PubMed: 18429699]

[33]. Canto C, Menzies KJ, Auwerx J. NAD(+) Metabolism and the Control of Energy Homeostasis: A Balancing Act between Mitochondria and the Nucleus. Cell Metab. 2015;22:31–53. [PubMed: 26118927]

[34]. Grozio A, Sociali G, Sturla L, Caffa I, Soncini D, Salis A, et al. CD73 protein as a source of extracellular precursors for sustained NAD+ biosynthesis in FK866-treated tumor cells. J Biol Chem. 2013;288:25938–49. [PubMed: 23880765]

[35]. Liu L, Su X, Quinn WJ 3rd, Hui S, Krukenberg K, Frederick DW, et al. Quantitative Analysis of NAD Synthesis-Breakdown Fluxes. Cell Metab. 2018;27:1067–80 e5. [PubMed: 29685734]

[36]. Langelier MF, Zandarashvili L, Aguiar PM, Black BE, Pascal JM. NAD(+) analog reveals PARP-1 substrate-blocking mechanism and allosteric communication from catalytic center to DNA-binding domains. Nat Commun. 2018;9:844. [PubMed: 29487285]

[37]. Michan S, Sinclair D. Sirtuins in mammals: insights into their biological function. Biochem J. 2007;404:1–13. [PubMed: 17447894]

[38]. Chini EN. CD38 as a regulator of cellular NAD: a novel potential pharmacological target for metabolic conditions. Curr Pharm Des. 2009;15:57–63. [PubMed: 19149603]

[39]. Burgos ES. NAMPT in regulated NAD biosynthesis and its pivotal role in human metabolism. Curr Med Chem. 2011;18:1947–61. [PubMed: 21517777]

[40]. Ratajczak J, Joffraud M, Trammell SA, Ras R, Canela N, Boutant M, et al. NRK1 controls nicotinamide mononucleotide and nicotinamide riboside metabolism in mammalian cells. Nat Commun. 2016;7:13103. [PubMed: 27725675]

[41]. Johnson S, Imai SI. NAD (+) biosynthesis, aging, and disease. F1000Res. 2018;7:132. [PubMed: 29744033]

[42]. Gressner AM, Weiskirchen R, Breitkopf K, Dooley S. Roles of TGF-beta in hepatic fibrosis. Front Biosci. 2002;7:d793–807. [PubMed: 11897555]

[43]. Murano I, Barbatelli G, Parisani V, Latini C, Muzzonigro G, Castellucci M, et al. Dead adipocytes, detected as crown-like structures, are prevalent in visceral fat depots of genetically obese mice. J Lipid Res. 2008;49:1562–8. [PubMed: 18390487]

[44]. Younossi ZM. Review article: current management of non-alcoholic fatty liver disease and non-alcoholic steatohepatitis. Alimentary pharmacology & therapeutics. 2008;28:2–12. [PubMed: 18410557]

[45]. Friedman SL. Hepatic stellate cells: protean, multifunctional, and enigmatic cells of the liver. Physiol Rev. 2008;88:125–72. [PubMed: 18195085]

[46]. Tsuchida T, Friedman SL. Mechanisms of hepatic stellate cell activation. Nat Rev Gastroenterol Hepatol. 2017;14:397–411. [PubMed: 28487545]

[47]. Tacke F, Zimmermann HW. Macrophage heterogeneity in liver injury and fibrosis. J Hepatol. 2014;60:1090–6. [PubMed: 24412603]

[48]. Bae M, Park YK, Lee JY. Food components with antifibrotic activity and implications in prevention of liver disease. J Nutr Biochem. 2018;55:1–11. [PubMed: 29268106]

[49]. Dominguez-Perez M, Simoni-Nieves A, Rosales P, Nuno-Lambarri N, Rosas-Lemus M, Souza V, et al. Cholesterol burden in the liver induces mitochondrial dynamic changes and resistance to apoptosis. J Cell Physiol. 2018.

[50]. Revollo JR, Grimm AA, Imai S. The NAD biosynthesis pathway mediated by nicotinamide phosphoribosyltransferase regulates Sir2 activity in mammalian cells. J Biol Chem. 2004;279:50754–63. [PubMed: 15381699]

[51]. Zhang H, Chen F, Fan X, Lin C, Hao Y, Wei H, et al. Quantitative Proteomic analysis on Activated Hepatic Stellate Cells reversion Reveal STAT1 as a key regulator between Liver Fibrosis and recovery. Sci Rep. 2017;7:44910. [PubMed: 28322315]

[52]. Bai P, Canto C, Oudart H, Brunyanszki A, Cen Y, Thomas C, et al. PARP-1 inhibition increases mitochondrial metabolism through SIRT1 activation. Cell Metab. 2011;13:461–8. [PubMed: 21459330]

[53]. Gariani K, Ryu D, Menzies KJ, Yi HS, Stein S, Zhang H, et al. Inhibiting poly ADP-ribosylation increases fatty acid oxidation and protects against fatty liver disease. J Hepatol. 2017;66:132–41. [PubMed: 27663419]

[54]. Mukhopadhyay P, Rajesh M, Cao Z, Horvath B, Park O, Wang H, et al. Poly (ADP-ribose) polymerase-1 is a key mediator of liver inflammation and fibrosis. Hepatology. 2014;59:1998–2009. [PubMed: 24089324]

[55]. Kim SY, Cho BH, Kim UH. CD38-mediated Ca2+ signaling contributes to angiotensin II-induced activation of hepatic stellate cells: attenuation of hepatic fibrosis by CD38 ablation. J Biol Chem. 2010;285:576–82. [PubMed: 19910464]

[56]. Li M, Hong W, Hao C, Li L, Wu D, Shen A, et al. SIRT1 antagonizes liver fibrosis by blocking hepatic stellate cell activation in mice. FASEB J. 2018;32:500–11. [PubMed: 28970250]

[57]. Sun L, Fan Z, Chen J, Tian W, Li M, Xu H, et al. Transcriptional repression of SIRT1 by protein inhibitor of activated STAT 4 (PIAS4) in hepatic stellate cells contributes to liver fibrosis. Sci Rep. 2016;6:28432. [PubMed: 27323886]

[58]. Wu Y, Liu X, Zhou Q, Huang C, Meng X, Xu F, et al. Silent information regulator 1 (SIRT1) ameliorates liver fibrosis via promoting activated stellate cell apoptosis and reversion. Toxicol Appl Pharmacol. 2015;289:163–76. [PubMed: 26435214]

[59]. Massague J TGFbeta signalling in context. Nat Rev Mol Cell Biol. 2012;13:616–30. [PubMed: 22992590]

[60]. Simonsson M, Kanduri M, Gronroos E, Heldin CH, Ericsson J. The DNA binding activities of Smad2 and Smad3 are regulated by coactivator-mediated acetylation. J Biol Chem. 2006;281:39870–80. [PubMed: 17074756]

[61]. Inoue Y, Itoh Y, Abe K, Okamoto T, Daitoku H, Fukamizu A, et al. Smad3 is acetylated by p300/CBP to regulate its transactivation activity. Oncogene. 2007;26:500–8. [PubMed: 16862174]

Highlights

- Nicotinamide riboside supplementation reduced liver fibrosis in mice
- Reduction of liver fibrosis is independent of steatosis and inflammation
- Fatty liver and activated hepatic stellate cells have altered NAD+ metabolism
- Nicotinamide riboside treatment reduced activation of hepatic stellate cells in vitro
- Nicotinamide riboside increased whole body energy expenditure to reduce weight gain

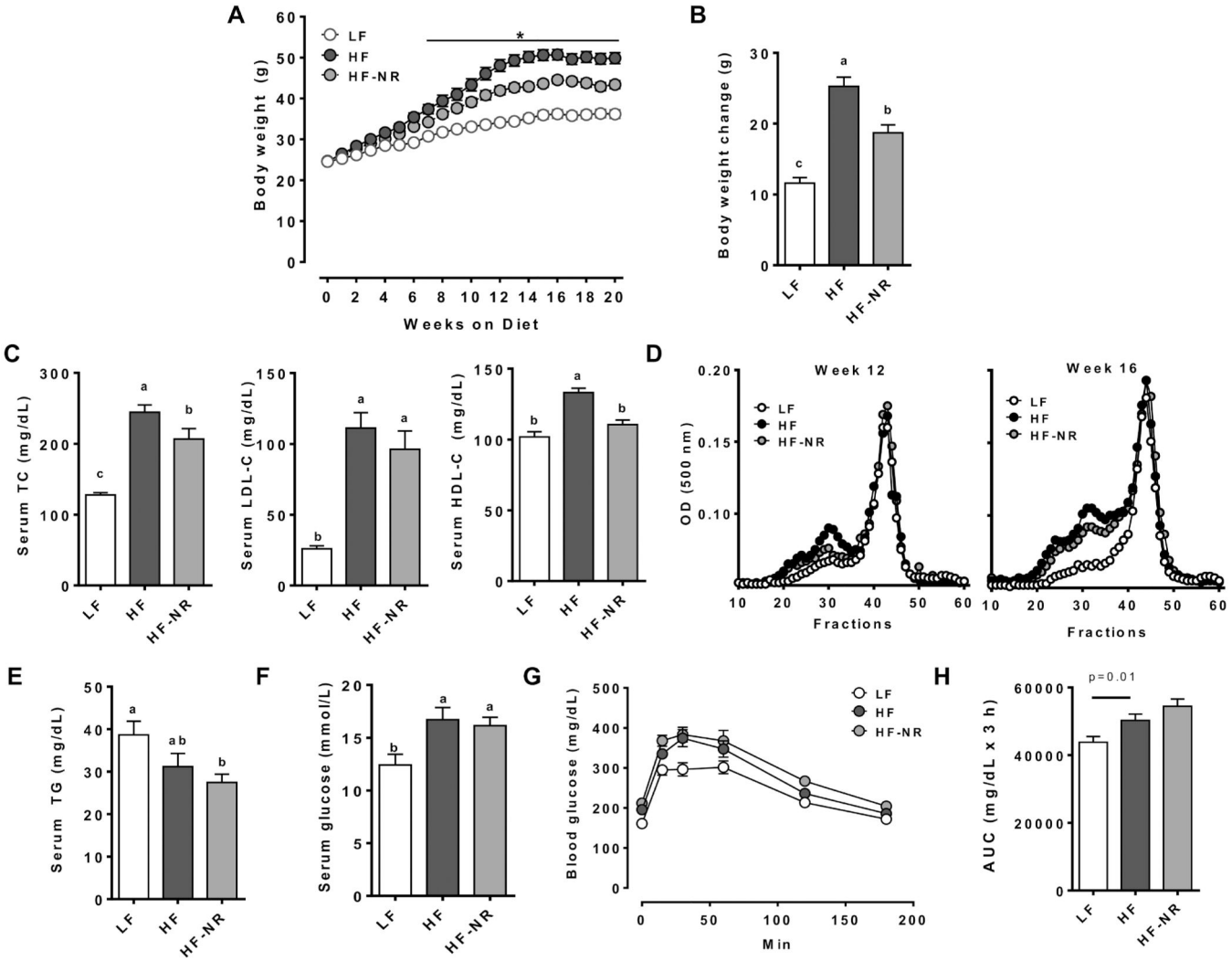

Figure 1.

NR supplementation lowered body weight and led to a more favorable lipid profile, but did not improve glucose tolerance. **A)** Body weight of mice through 20 weeks of experimental diets. **B)** Body weight change. **C)** Serum total cholesterol, LDL-cholesterol, HDL-cholesterol. **D)** Lipoprotein profile of pooled plasma of mice from each group. **E)** Serum triglycerides. **F)** Serum glucose. **G)** Oral glucose tolerance test. **H)** Area under the curve of OGTT. n =13–15 per group. Data shown are mean ± SEM. Bars with different letters are significantly differently from each other. * indicates significantly different between HF and HF-NR. ($p < 0.05$)

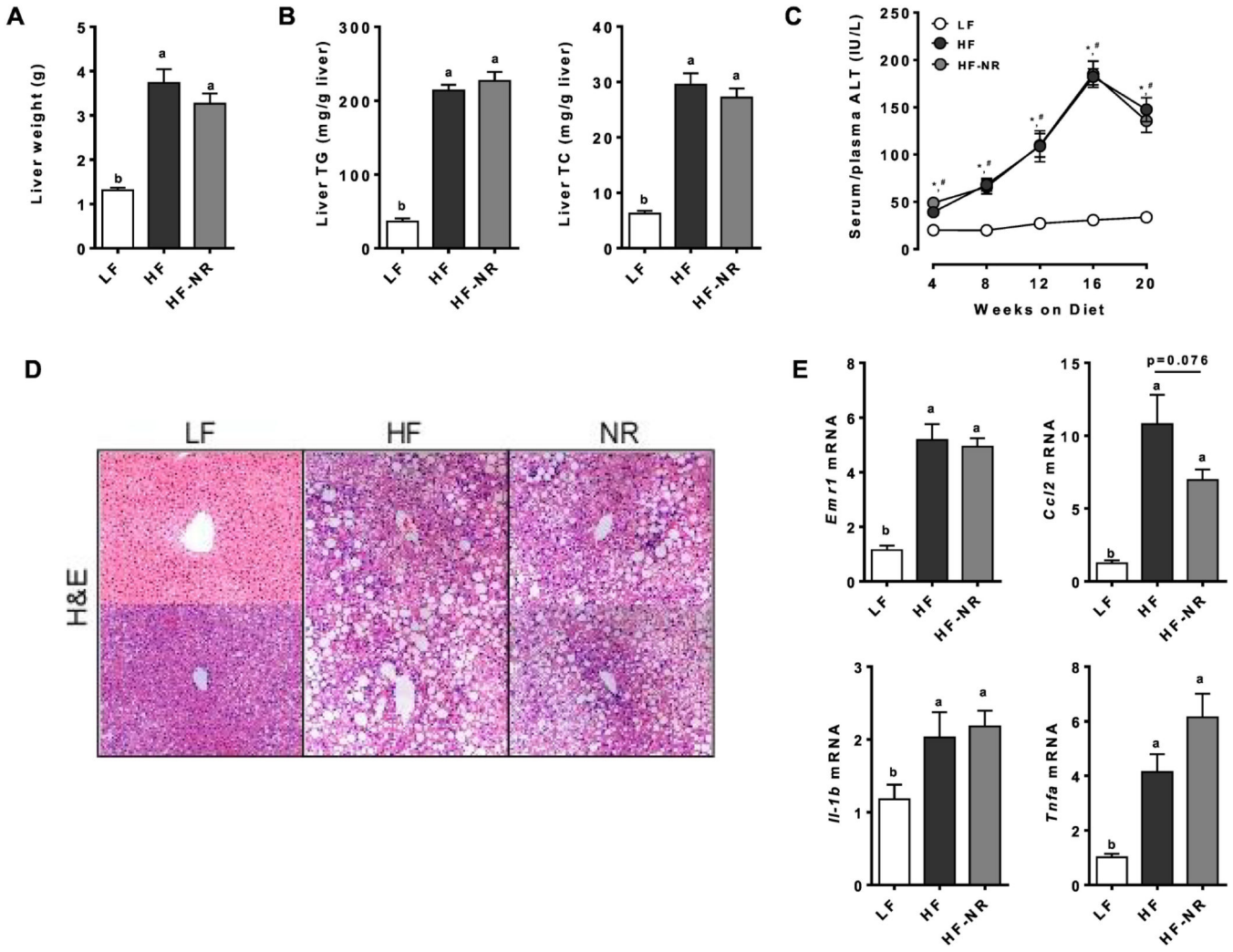

Figure 2.

NR did not reduce TG and TC accumulation or inflammation in the liver. **A)** Liver weight. **B)** Liver triglyceride and total cholesterol. **C)** Plasma ALT at wk 4–16 and serum ALT at wk 20. * significance between LF and HF, # indicates significance between LF and HF-NR. **D)** Representative picture of hematoxylin and eosin (H&E) staining of liver sections from 2 different mice in each group. **E)** Liver mRNA expression of inflammatory genes. n =13–15 per group. Data shown are mean ± SEM. Bars with different letters are significantly different from each other. ($p < 0.05$)

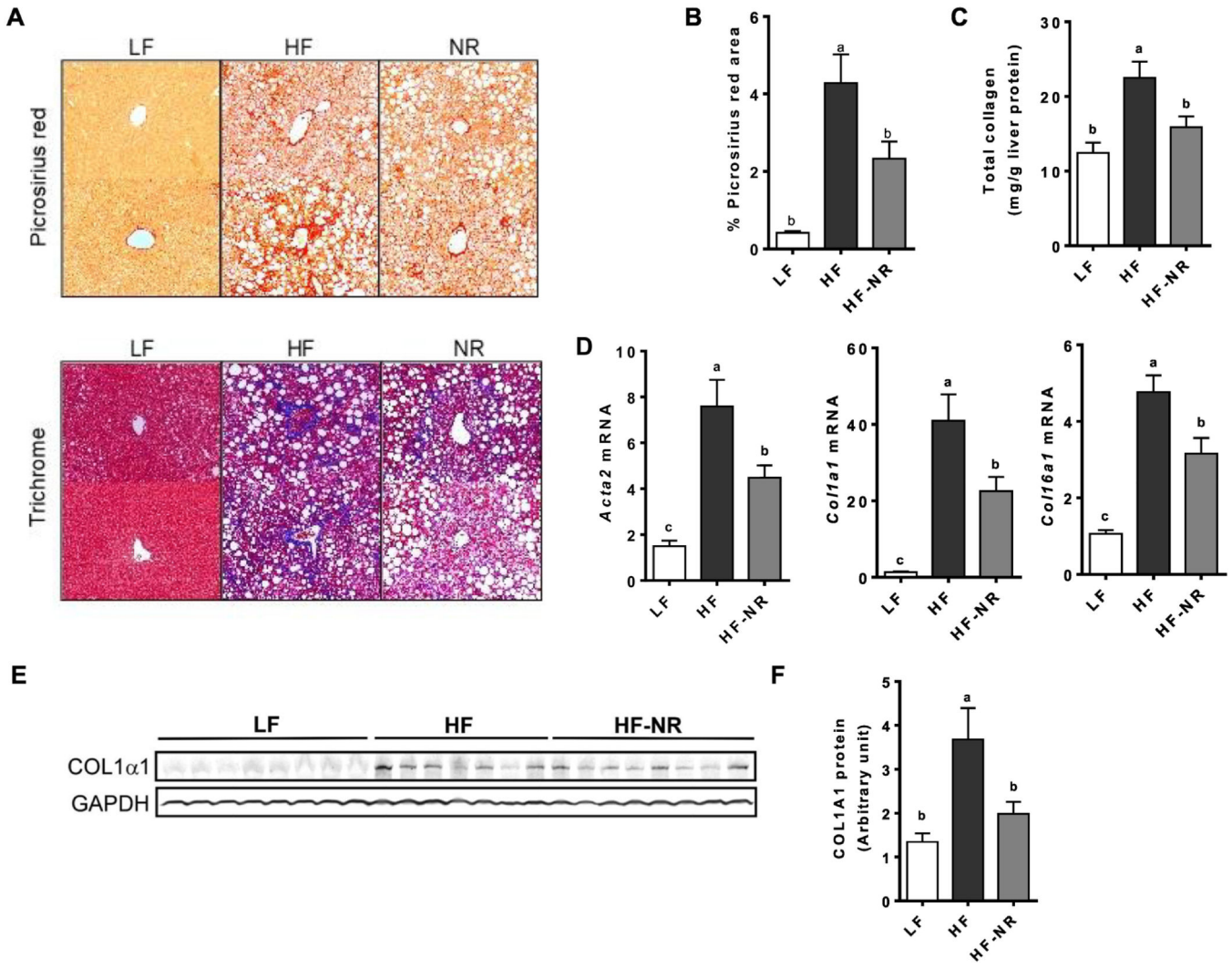

Figure 3.

NR supplementation reduced collagen accumulation in the liver. **A)** Representative picture of picrosirius red staining (top) and trichrome staining (bottom) of liver sections from 2 different mice in each group. **B)** Quantification of picrosirius red positive area. **C)** Total liver collagen quantification. **D)** Liver mRNA expression of fibrotic genes. **E)** Representative Western blot of COL1α1 in the liver of mice from each group. **F)** Quantification of COL1α1 protein level. n =13–15 per group. Data shown are mean ± SEM. Bars with different letters are significantly different from each other. ($p < 0.05$)

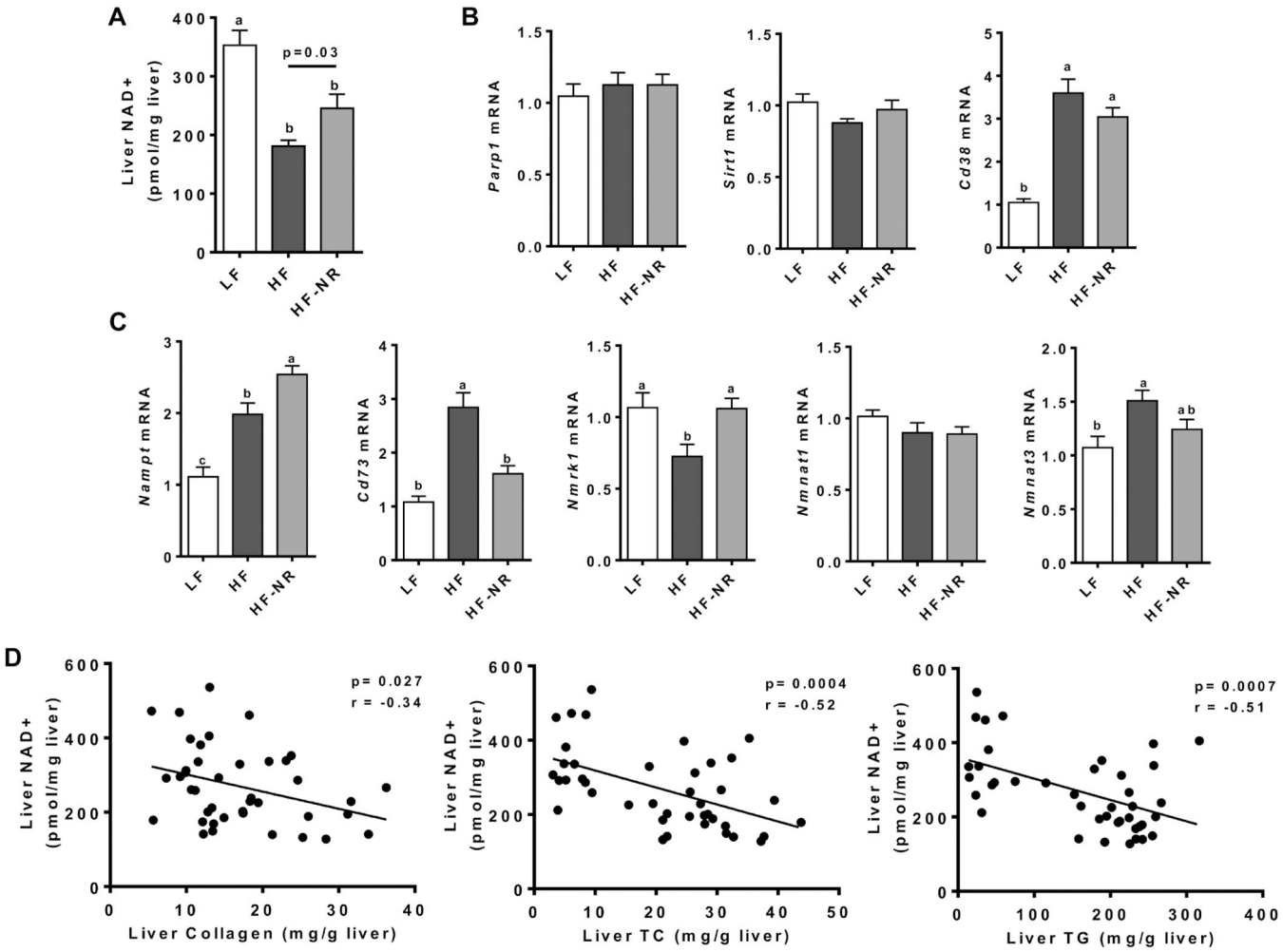

Figure 4.

HF altered liver NAD+ metabolism which is attenuated by NR supplementation. **A)** Quantification of liver NAD+ by enzyme cycling assay. **B)** Liver mRNA expression of known NAD+ consuming enzymes. **C)** Liver mRNA expression of genes involved in the NAD+ salvage pathway. **D)** Correlation analysis of liver NAD+ concentration with liver collagen, total cholesterol, and triglycerides. n =13–15 per group. Data shown are mean ± SEM. Bars with different letters are significantly different from each other. ($p < 0.05$)

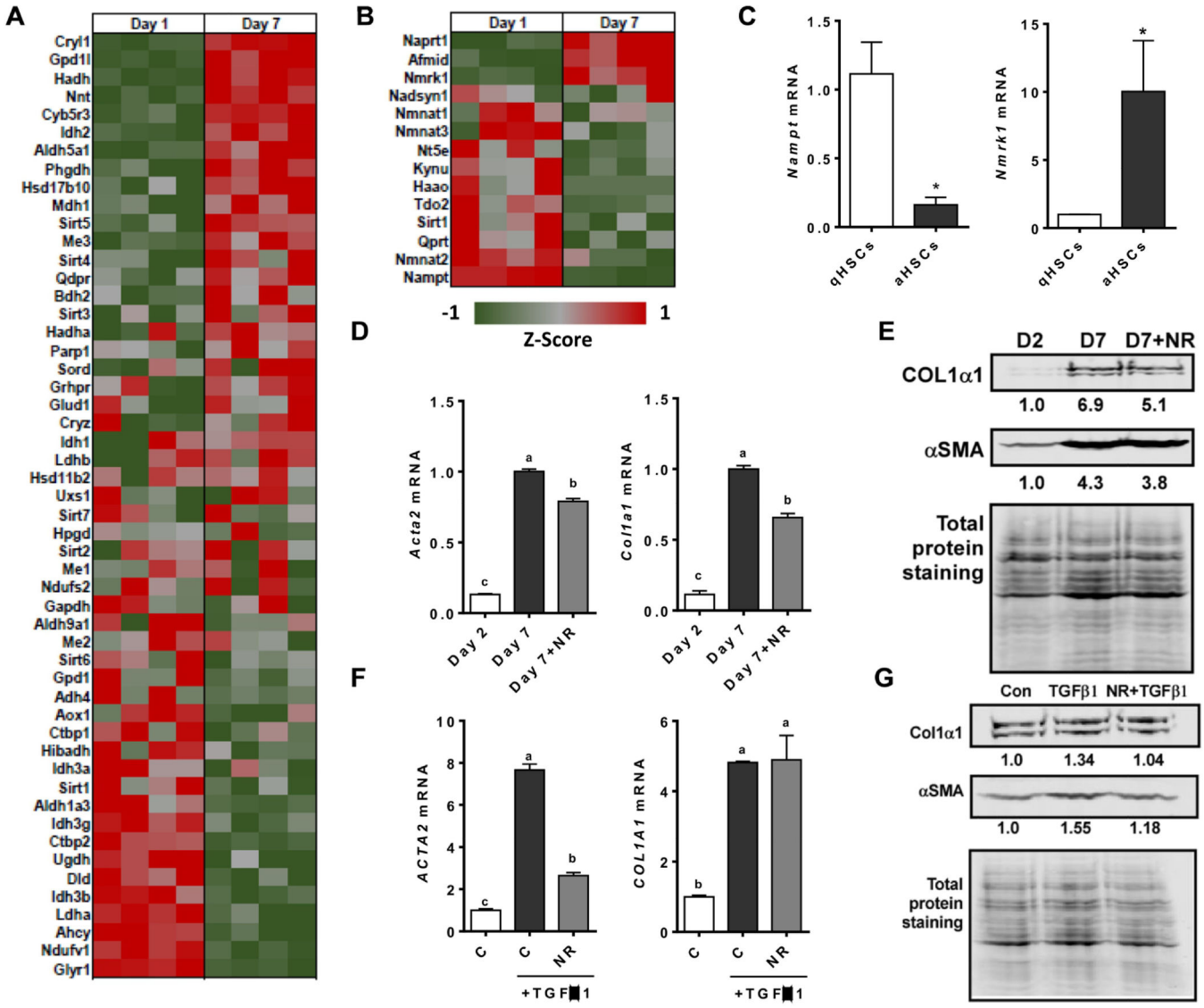

Figure 5.

NAD+ metabolism is altered in activated HSCs and NR treatment can attenuate the activation of hepatic stellate cells. **A)** Heat map of genes from RNA-Seq requiring NAD+ as a cofactor in quiescent HSCs (day 1) and activated HSCs (day 7). **B)** Heat map of genes from RNA-Seq of NAD+ de novo biosynthesis and salvage pathway in quiescent HSCs (day 1) and activated HSCs (day 7). **C)** mRNA expression of Nmrk1 and Nampt1 in mouse primary HSCs at day 1 and day 7. **D)** mRNA expression of primary mouse HSCs treated with or without 1.0 mM NR from day 2 to day 7. **E)** Representative Western blot analysis of mouse primary HSCs treated with or without 1.0 mM NR from day 2 to day 7 and normalized with total protein staining. The result of quantification is shown under each protein band. **F)** mRNA expression and **G)** Western blot analysis of primary human HSCs pretreated with 1.0 mM NR for 6 hours and then treated with 2 ng/mL of TGFβ1 for 24 h. The result of quantification is shown under each band. Data shown are mean ± SEM. Bars with different letters are significantly different from each other. ($p < 0.05$)

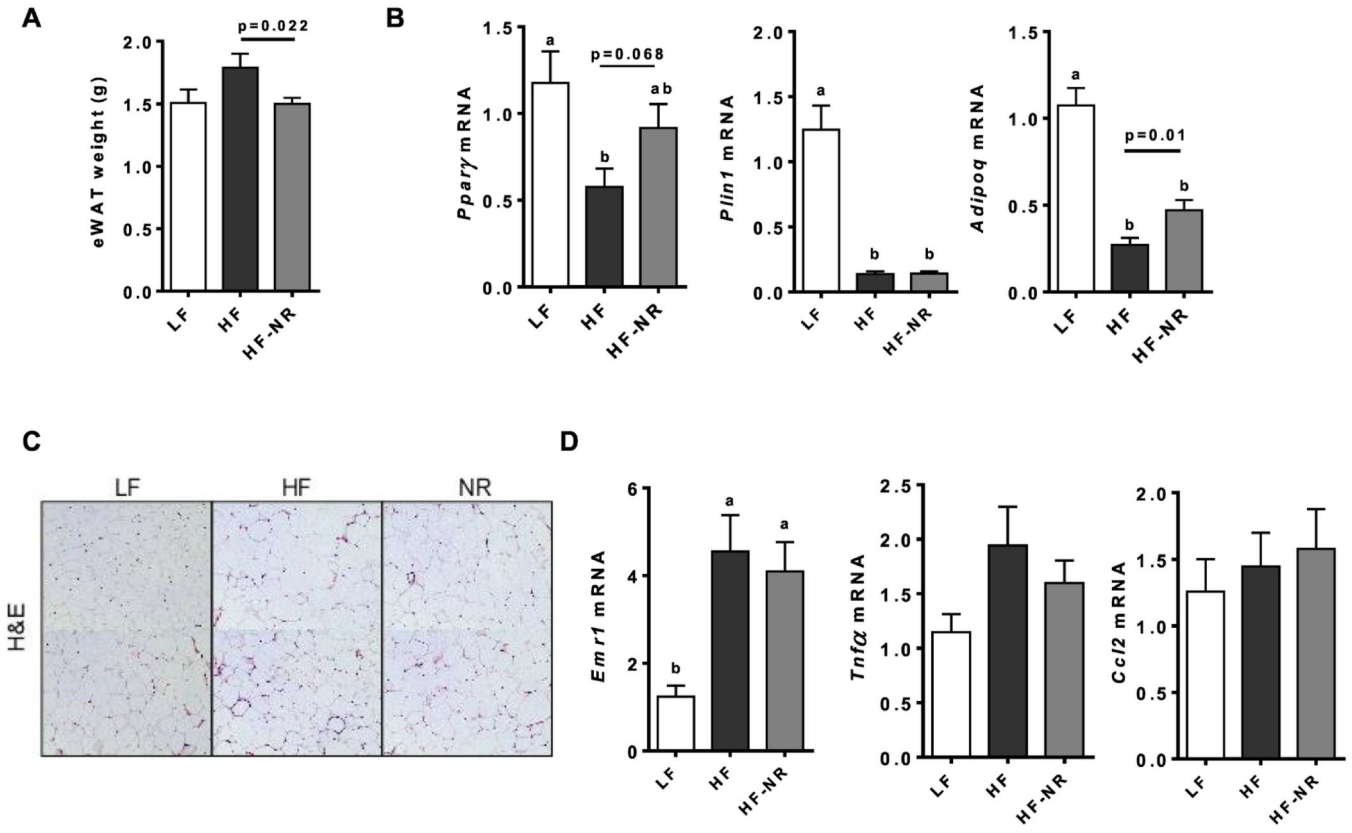

Figure 6.

NR did not increase energy utilization gene expression in epididymal fat pad, but reduced its weight. **A)** epididymal white adipose tissue (eWAT) weight. **B)** eWAT mRNA expression of adipogenic genes. **C)** Representative images of hematoxylin and eosin staining of eWAT sections. **D)** eWAT mRNA expression of inflammatory genes. n =13–15 per group. Data shown are mean ± SEM. Bars with different letters are significantly different from each other. ($p < 0.05$)

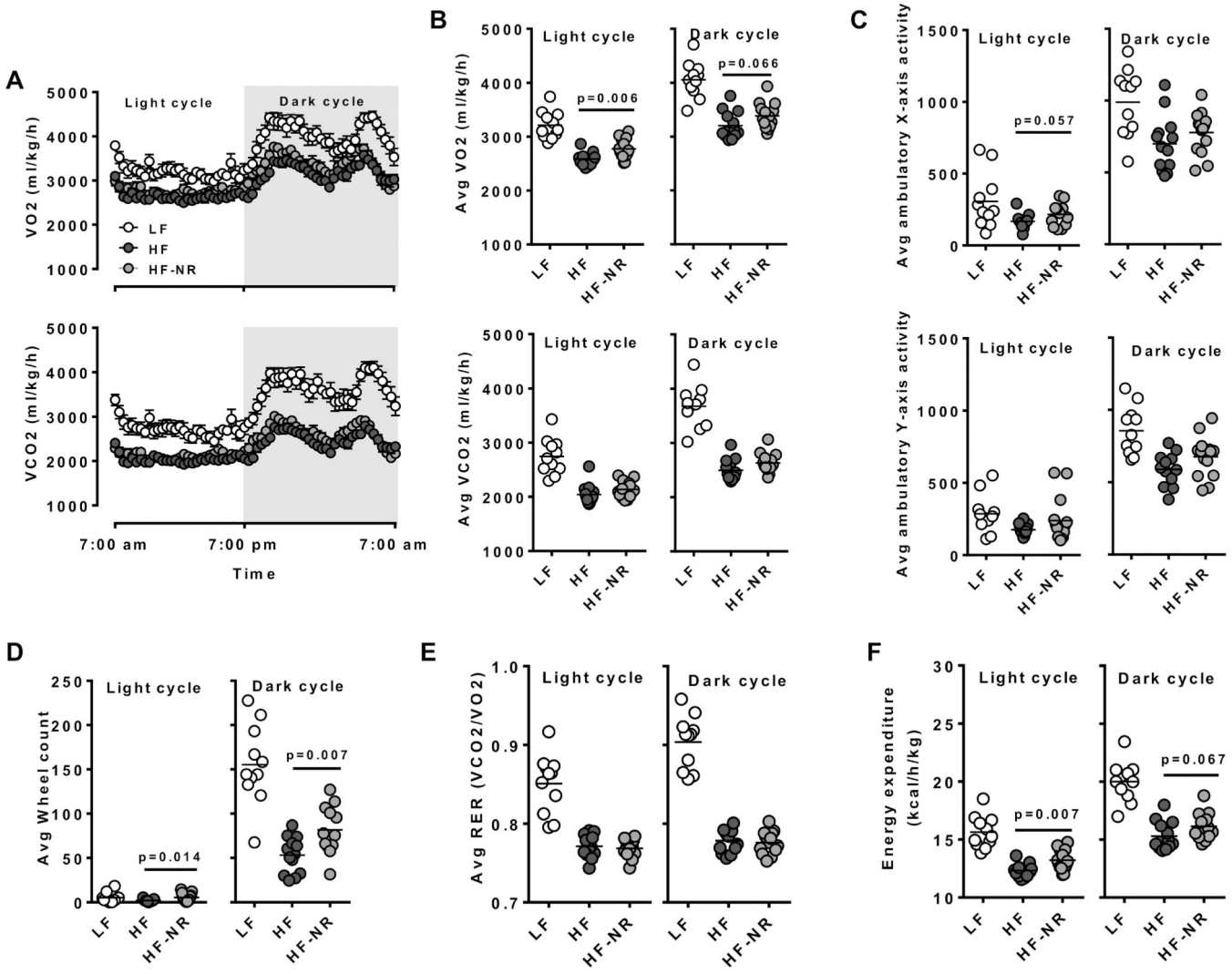

Figure 7.

NR increase whole body energy utilization in mice. Indirect calorimetry measurement of mice metabolism. **A)** O_2 consumption (top) and CO_2 production (bottom) rate during light and dark cycle over a 24 h cycle. **B)** Average O_2 consumption (top) and CO_2 production (bottom) rate during light and dark cycle. **C)** Average ambulatory X and Y movement in light and dark cycles. **D)** Average running wheel use. **E)** Average respiratory exchange ratio (RER) of mice in light and dark cycle. **F)** Mice energy expenditure in light and dark cycle. n=11–15. Data shown are mean ± SEM. Bars with different letters are significantly different from each other ($p < 0.05$)

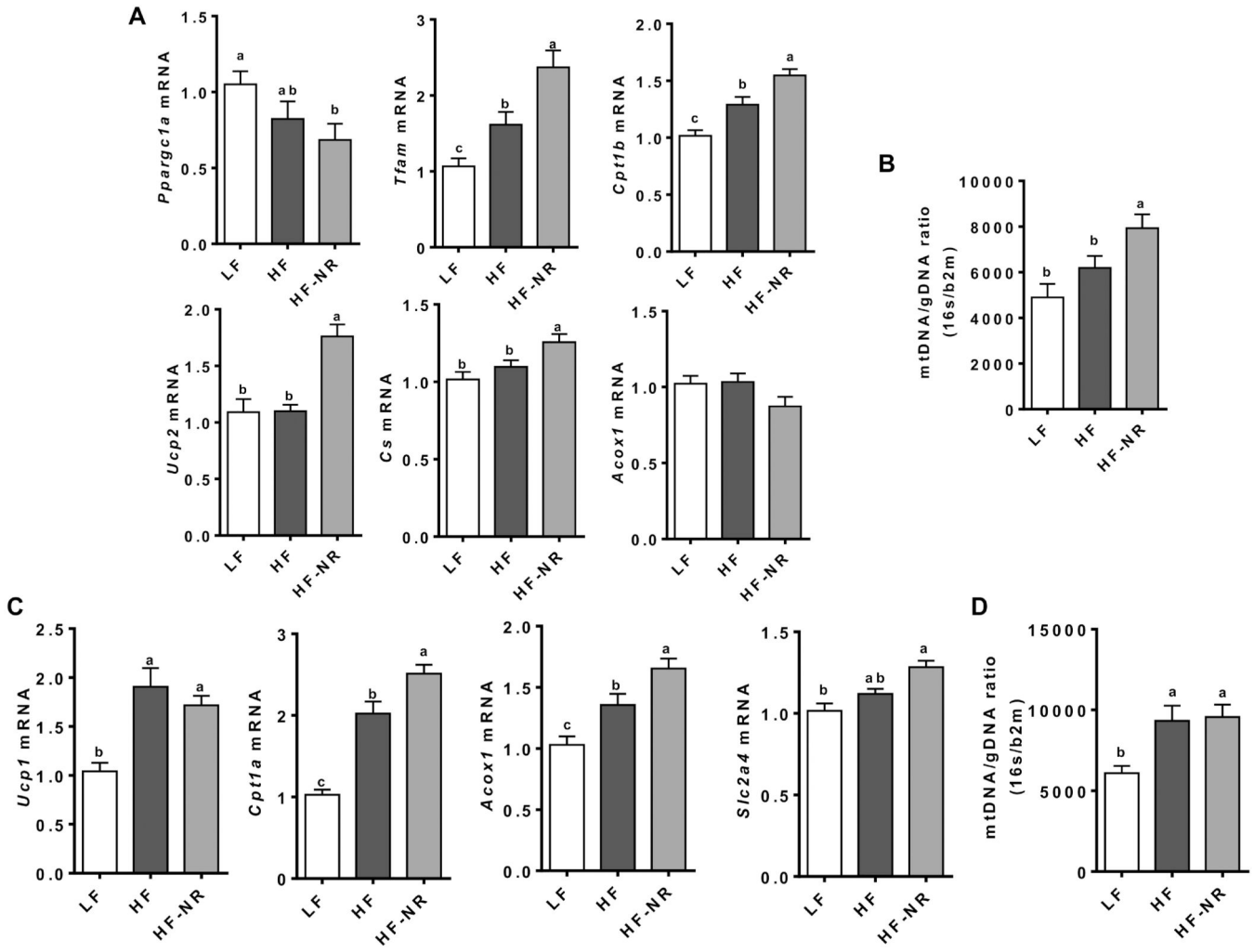

Figure 8.

NR increase energy utilization genes in soleus muscle and brown adipose tissue. **A)** mRNA expression of β-oxidation and mitochondria biogenesis genes in soleus muscle. **B)** mitochondria DNA quantification in soleus muscle. The ratio of 16s RNA and β−2-microglobulin. **C)** mRNA expression of β-oxidation and glucose utilization genes in brown adipose tissue. **D)** mitochondria DNA quantification in brown adipose tissue. The ratio of 16s RNA and β−2-microglobulin.